NACA

RESEARCH MEMORANDUM

TURBINE-ROTOR-BLADE DESIGNS BASED ON

ONE-DIMENSIONAL-FLOW THEORY

I - PERFORMANCE OF SINGLE-STAGE TURBINE

HAVING 40-PERCENT REACTION

By Robert E. English and Cavour H. Hauser

Lewis Flight Propulsion Laboratory
Cleveland, Ohio

NATIONAL ADVISORY COMMITTEE
FOR AERONAUTICS
WASHINGTON
June 10, 1949

NATIONAL ADVISORY COMMITTEE FOR AERONAUTICS

RESEARCH MEMORANDUM

TURBINE-ROTOR-BLADE DESIGNS BASED ON ONE-DIMENSIONAL-FLOW THEORY

I - PERFORMANCE OF SINGLE-STAGE TURBINE

HAVING 40-PERCENT REACTION

By Robert E. English and Cavour H. Hauser

SUMMARY

As part of a research program to determine design criterions for aircraft gas turbines with high efficiency and high pressure ratio per stage, the NACA is investigating a family of turbine-rotor-blade designs based on one-dimensional-flow theory and incorporating systematic changes in design variables. The rotor blade described herein was designed for a total-to-static pressure ratio of 4.00 and 40-percent reaction. The static pressure was assumed constant along the radius at the entrance and the exit of each row of blades. The rotor-blade passage was based on one-dimensional-flow theory. The convex surface of the blade was assigned to be the involute of a circle and the channel width was determined from continuity considerations by assuming that the drop in static enthalpy along the mean flow path of the channel is proportional to the square of the distance from the channel entrance.

The performance investigation of this design in an experimental cold-air turbine yielded the following results: The maximum brake internal efficiency in the region of the design point was slightly greater than 0.84, and a brake internal efficiency of 0.81 was obtained for all total-pressure ratios from 1.25 to 3.80. At the equivalent mean blade speed and total-to-static pressure ratio for which the blades were designed, the brake internal efficiency was 0.82. The maximum brake net and brake internal efficiencies occurred at blade-to-jet speed ratios between 0.48 and 0.55. Measured static pressures in the exhaust annulus showed that, contrary to the design assumption, the static pressure varied 5 percent at the design conditions.

INTRODUCTION

As part of a research program to establish design criterions
for aircraft gas turbines with high efficiency and high pressure
ratio per stage, a series of turbine-rotor-blade designs based on
one-dimensional-flow theory and incorporating systematic changes
in the design variables is being investigated at the NACA Lewis
laboratory. The same stator design will be used throughout the
program.

The performance of one particular blade design is reported
herein. The general assumptions applicable to all the blade
designs together with the features of the particular design are
listed. The blades reported herein are identified by a design
reaction of 40 percent, a suction (convex) surface contour that is
the involute of a circle, a static-enthalpy drop through the rotor
blades proportional to the square of the distance from the channel
entrance measured along the flow-path length, and a solidity based
on the axial width of 2.2 at the mean radius.

The performance of these turbine-blade designs is being inves-
tigated in an experimental single-stage turbine with entrance con-
ditions of atmospheric pressure and a temperature of 710° R. Per-
formance data for the set of blades described herein have been
obtained over a range of equivalent mean blade speeds from 190 to
807 feet per second and total-pressure ratios from 1.18 to 3.80,
which includes the design values of equivalent mean blade speed
and total-pressure ratio of 643 feet per second and 3.32, respec-
tively.

Over-all turbine performance is presented in the form of a
composite plot that shows the effect of equivalent mean blade
speed and total-pressure ratio on the equivalent weight flow, the
brake internal efficiency, and the equivalent turbine-shaft work.
The variation of brake internal efficiency with blade-to-jet speed
ratio is plotted for two selected values of total-pressure ratio.
For the same two values of total-pressure ratio, a comparison
between brake internal efficiency and brake net efficiency is made
over the full range of blade-to-jet speed ratios. In the blade
design, constant static pressure along the radius was assumed at
the stator entrance, the stator exit, the rotor entrance, and the
rotor exit, which would result from small radial accelerations.
The weight flow per unit of annulus area was also assumed to be
constant in any plane normal to the axis of rotation. The dif-
ference between the actual and theoretical static-pressure distri-
bution along the radius at the rotor exit is presented.

SYMBOLS

The following symbols are used in this report:

a   velocity of sound, (ft/sec)

E   turbine-shaft work, (Btu/lb)

g   standard acceleration due to gravity, 32.17 (ft/sec^2)

h   specific enthalpy, (Btu/lb)

J   mechanical equivalent of heat, 778.3 (ft-lb/Btu)

p   absolute pressure, (lb/sq ft)

T   absolute temperature, (^{O}R)

U   mean blade speed, (ft/sec)

V   absolute velocity of gas, (ft/sec)

V_j ideal jet velocity, (ft/sec)

W   gas velocity relative to rotor, (ft/sec)

w   weight flow, (lb/sec)

α   angle of absolute velocity measured from direction of blade motion, (deg)

β   angle of relative velocity measured from direction of blade motion, (deg)

η_i brake internal efficiency

η_{net} brake net efficiency

ν ratio of mean blade speed to ideal jet velocity

ρ   mass density, (slugs/cu ft)

Subscripts:

0   NACA sea-level air; 2116 (lb/sq ft); 518.4 (^{O}R)

1   stator entrance

2   stator exit

3   rotor entrance

4   rotor exit

h   inner radius

s   isentropic

T   outer radius

u   tangential component

x   axial component

Superscript:

'   total, or stagnation, state

TURBINE DESIGN

In the turbine-rotor-blade investigations, the four variables considered are: the amount of reaction, the shape of the suction surface of the blades, the distribution of the enthalpy drop through the blade passages, and the blade solidity. The blades reported herein are identified by a design reaction of 40 percent, a convex-surface contour that is the involute of a circle, a static-enthalpy drop through the rotor blades proportional to the square of the distance from the channel entrance measured along the flow path, and a solidity based on the axial width of 2.2 at the mean radius. The amount of reaction is defined as $\left[(h_3-h_4) \, / \, (h'_1-h_4) \right]_s$.

The following conditions and assumptions apply at the design point to all the blades in the series:

Conditions:

Entrance total temperature, T'_1, °R 1960

Entrance total pressure, p'_1, lb/sq ft 2829

in. Hg 40.0

Mean blade speed, U, ft/sec 1210

Total-to-static pressure ratio, p'_1/p_4 . . . . 4.00

Stator-exit angle (constant over blade height), α_2, deg . . . 20

Assumptions:

(1) The total pressure and the total temperature are uniform over the blade height at the entrance to the stator.

(2) The expansion in the turbine is adiabatic.

(3) In any plane normal to the axis of rotation, the weight flow per unit radius is proportional to the radius; at stator entrance, stator exit, rotor entrance, and rotor exit (stations 1, 2, 3, and 4, respectively), this condition produces constant weight flow per unit of annular area.

(4) At stator entrance, stator exit, rotor entrance, and rotor exit (stations 1, 2, 3, and 4, respectively), the static pressure is constant along the radius. This assumption produces constant resultant velocity V_2 along the radius, which, according to reference 1 (p. 146), may be assumed. It is thus assumed that only small radial accelerations will be encountered.

(5) In the stator, the static pressure at the exit from the passages between the blades is the critical pressure and further expansion with an accompanying acceleration to supersonic velocities takes place downstream of these passages. For the acceleration beyond sonic velocity, the stream does not deflect toward the axial direction with the result that the absolute velocity at the rotor entrance V_3 is at the angle of the trailing edges of the stator blades; the increase in flow area required for the supersonic acceleration is obtained from a reduction in the thickness of the wakes downstream of the trailing edges of the stator blades.

(6) In the rotor blade passage, expansion takes place until critical conditions are obtained unless the assigned amount of reaction is so low that the exit static pressure is greater than the critical pressure in the rotor. When critical conditions are obtained within the rotor-blade passage, the point at which choking occurs is made the passage exit. Expansion takes place downstream of the passage to the rotor-exit pressure in the same manner as the supercritical expansion for the stator. The relative velocity at the rotor exit is at the angle of the trailing edges of the rotor blades, which was calculated to maintain continuity of flow through the rotor blade passage.

(7) The velocity coefficient (ratio of actual to ideal velocity) for the stator is 0.985. (See reference 2.)

(8) In the rotor, the flow losses reduce the exit kinetic energy $W_4{}^2/2gJ$ by 3 Btu per pound, a value chosen arbitrarily.

(9) For the combustion products that constitute the working fluid, the ratio of specific heats is 1.300, and the specific heat at constant pressure is 0.300. The gas constant for a perfect gas having these properties is 53.9 foot-pounds per pound °R.

These restrictions determine the vector diagram for the turbine. The diagram for the mean section of the blade discussed is shown in figure 1. The conditions of constant angle of flow and constant static pressure along the radius at the rotor entrance produce an absolute velocity that is constant in both direction and magnitude along the radius.

The turbine design performance for the blade design discussed reduced to NACA sea-level conditions at the turbine entrance is as follows:

Equivalent mean blade speed, $U(a_0/a'_1)$, ft/sec 643

Equivalent weight flow, $w\left(\dfrac{\rho_0 a_0}{\rho'_1 a'_1}\right)$, lb/sec 5.82

Blade-to-jet speed ratio, U/V_J 0.43

Equivalent work output, $E(a_0/a'_1)^2$, Btu/lb 34.8

Total-to-static pressure ratio, p'_1/p_4 . . . . 4.00

Net efficiency 0.77

If the exit total pressure is determined by adding to the static pressure a dynamic pressure corresponding to the axial component of the design exit velocity $V_{x,4}$, the total-pressure ratio p'_1/p'_4 is 3.32 and the internal efficiency is 0.92. If the exit total pressure is determined by adding to the static pressure a dynamic pressure corresponding to the resultant exit velocity V_4, the internal efficiency is 0.96.

Stator Blades

A single stator design will be used for the whole series of rotor blades. The stator blades were formed from stampings of

1/16-inch sheet steel. The profile at the mean section is shown in figure 2. The mean line of the blade profile had a short straight axial section AB. The mean line from B to C was made up of three arbitrary circular arcs of increasing radius. The rest of the mean line from C to D was straight and tangent to the curved section at point C. The geometry of the stator assembly is shown in figure 3; the blades were so mounted that the leading edge was set at an angle of 14° from a radial line through the leading edge of the root section and the trailing edge was set at an angle of 24° from a radial line through the trailing edge of the root section. The blades were first stamped to shape; then the leading edges were rounded to form a 0.062-inch-radius cylinder and the trailing edge was reduced to 0.031 inch as shown in figure 2. The nominal 0.031-inch trailing-edge thickness was slightly and irregularly reduced in the stator blades used in this investigation owing to hand-finishing that was necessitated by mechanical damage to this stator. The curved portion of the blade from B to C was constant over the blade height; but the length AB varied from 0.083 inch at the root section to 0.031 inch at the tip, and the distance CD varied from 0.971 inch at the root section to 1.185 inches at the tip section. This variation in contour from root to tip was made necessary by the assigned angles of 14° and 24° between radial elements and the leading and trailing edges, respectively. The stator-blade height was made equal to the rotor-blade height at the rotor entrance. In order to complete the stator assembly, 36 of these blades were welded to two concentric, cylindrical rings; the fillets thus formed at the roots and the tips of the blades were hand-finished to provide smooth flow passages.

Rotor Blades

The rotor-blade profiles at the root, mean, and tip sections of the blade discussed herein were designed in a manner similar to that shown for the mean section in figure 4. An involute of a circle was arbitrarily selected as the part of the suction surface between points A and B. The involute of a circle, which provides the suction surface with a gradually increasing radius of curvature, reduces the magnitude of any decrease in velocity along the suction surface such as might be caused by the combination of a circular arc and a straight line. From the downstream end of the involute (point A, fig. 4) the contour was faired to meet the straight line that extends from E to the trailing-edge circle. Upstream of the involute, the suction surface was faired from point B to the leading-edge circle.

In the entrance region of the rotor cascade immediately
upstream of the guided channel ABCDEA, the gas was assumed to turn
between 15° and 20° toward the axial direction without changing the
magnitude of the relative velocity. This assumption gave the nose
of the blade a small angle of attack, which aided in extending the
range of efficient operation of the design. (See reference 1,
p. 145.)

The pressure (concave) surface of the rotor blades was deter-
mined from one-dimensional-flow theory by considering the guided
channel ABCDEA between two blades as a curved nozzle for which the
specific mass flow on the center line is the average for the chan-
nel. For each point Y on the suction surface of the blade, there
was a corresponding point Z on the channel center line through
which a line passed that was normal to the suction surface. At
any point Z along the channel center line for which the channel
area is greater than the channel exit area, the ratio of the ideal
change in static enthalpy from the entrance of the guided channel
to the ideal change in static enthalpy across the rotor was made
equal to the square of the ratio of the distance, measured along
the suction surface, of the point Y from the entrance of the guided
channel to the total channel length from B to E. Downstream of the
point at which the channel area became equal to the channel exit
area, the area was kept constant; the expansion beyond sonic speed
was assumed to take place without loss downstream of the channel.
The 3-Btu loss in the rotor was distributed in the following manner:
the actual change in static enthalpy to any point Z was assumed to
be lower than the ideal change in static enthalpy by an amount pro-
portional to the distance of the point Y from the entrance of the
guided channel. A side view of the blade mounted in the wheel is
shown in figure 5. The annular area was increased linearly from
the entrance to the exit of the rotor by having the annular walls
at the inner and outer radii make angles of 2° 17' and 3° 58',
respectively, with the axial direction. The flow was considered to
fill the channel at all points. At each of 10 stations in the
guided channel ABCDEA (fig. 4), the channel width at point Z sat-
isfying the above conditions was laid off normal to the suction
surface. The lines BC and DE were constructed normal to the rela-
tive velocities at the entrance and the exit of the guided channel,
respectively. The trailing-edge thickness was set at 0.030 inch.
The root, mean, and tip sections are superimposed in figure 6 to
show the relation among the sections and the general character of
the whole blade. The blades had very little twist or change in
camber from root to tip.

The turbine wheel was made up of 150 blades that were
1.47 inches long; the mean diameter at the midaxial-width plane was

13.25 inches and the outer wheel diameter was 14.75 inches. The
axial clearance between the trailing edge of the stator and the
leading edge of the rotor was 0.18 inch and the clearance between
the rotor blade exit and the downstream guide shells was 0.05 inch.
(See fig. 5.) Each blade was made with an integral cap at the tip,
so that with the blades clamped between two disks the caps formed
a continuous, rotating shroud. (See fig. 7.) A cylindrical sta-
tionary shroud was used to control leakage past the tips of the
rotor blades (fig. 5). The shroud was the same width as the blade
caps and the radial clearance between the blade caps and the shroud
was 0.025 inch or 0.017 of the blade height. Leakage past a shroud
of this type is shown in reference 3 to have a small effect on
performance.

For the investigation with cold air, the rotor blades used in
the turbine were made of die-cast aluminum. In the process of
manufacture, unavoidable errors were introduced, probably owing to
nonuniform shrinkage of the blade while cooling in the mold. Pro-
files of sample finished blades were inspected and compared with
the original blade design. For the blades reported herein, the
maximum deviation of the actual blade channel width from the design
width was less than 4.5 percent of the passage width. The exit
angle of the rotor blades was found to be within 2° of the design
exit angle β_4.

APPARATUS AND PROCEDURE

Experimental Equipment and Procedure

For this investigation, air from the test cell was used to
operate the turbine. The air was drawn through an electrostatic
precipitator that removed foreign material. In order to avoid
water condensation in the turbine, the filtered air was heated by
passing through a thermostatically controlled air heater. After
passing through the turbine, the air was exhausted by the laboratory
low-pressure exhaust system. The power output of the turbine was
absorbed by a water brake that was cradle-mounted for torque meas-
urement. A more detailed description of the experimental equipment
is given in reference 3.

Data were taken at 17 values of total-pressure ratio from
1.18 to 3.80 and at rotative speeds from 3880 to 16,490 rpm (equiv-
alent mean blade speeds from 190 to 807 ft/sec). At each of the
17 pressure ratios, the turbine was operated at 17 rotor speeds
with the exception of 11 data points at the lowest value of pres-
sure ratio and the higher blade speeds at which the turbine could

produce no shaft power. For all runs, the entrance total tempera-
ture was maintained between 708° and 712° R; the stator-entrance
total pressure varied between 26 and 29 inches of mercury, depend-
ing upon the air flow and local barometric pressure.

Instrumentation

A cross section of the turbine showing the instrumentation is
presented in figure 8. Entrance total pressure was indicated by a
total-pressure tube 0.75 inch upstream of the stator blades; a cir-
cumferential and radial total-pressure survey at the stator inlet
was made to insure that this tube indicated the average entrance
total pressure. The entrance total temperature was measured with
calibrated thermocouples at four stations in a pair of 20-inch-
diameter ducts leading to a plenum chamber immediately upstream of
the stator blades. The rotor-exit static pressure was measured
with 12 wall taps located 0.72 inch downstream of the rotor, six
on the inner exhaust-guide shell and six on the outer exhaust-guide
shell, evenly spaced circumferentially. The exit total temperature
was measured with three total-temperature-type thermocouples at the
downstream end of the two exhaust-guide shells. Although the
temperature variation along the radius may have prevented these
thermocouples from accurately indicating an average temperature, the
effect on turbine performance is small because, in accordance with
the manner in which these data were used, an error of 5° R would
change the computed internal or net efficiency less than 0.003.

Torque was measured with a commercial springless dynamometer
scale. Air flow was measured with a submerged 7-inch flat-plate
orifice upstream of the air heater. Turbine speed was indicated
by a calibrated electric tachometer.

The instruments were read with the following precision:

(1) Absolute pressure, ±0.05 inch of tetrabromoethane
        (acetylene tetrabromide)

(2) Temperature, ±1° R

(3) Orifice pressure drop, ±0.05 inch of water

(4) Torque load, ±0.2 pound

(5) Rotative speed, ±13 rpm

The minimum orifice pressure drop was 15 inches of water and the
minimum rotative speed, 3940 rpm. For a total-pressure ratio of
2.00 or greater, the torque load was at least 25 pounds, and the
maximum variation and the probable variation in the brake efficiency
were 0.018 and less than 0.005, respectively. For total-pressure
ratios less than 2.00, the errors in measurement of pressure and
torque cause the maximum and probable variations in efficiency to
exceed these values; these variations are inversely proportional to
the torque load and, roughly, the pressure drop across the turbine.

PERFORMANCE CALCULATIONS

Two separate efficiencies were determined to express the per-
formance of the turbine. The brake internal efficiency, which is
based on expansion between the entrance and exit total pressures,
is defined as

$$\eta_i \equiv \frac{E}{\left(h'_1 - h'_4\right)_s}$$

where E is the turbine-shaft work. The ideal drop in enthalpy
$\left(h'_1 - h'_4\right)_s$ was computed from the chart of air properties in refer-
ence 4, the values of entrance total pressure and temperature, and
the value of exit total pressure. The exit total pressure was
computed by adding to the measured static pressure a dynamic pres-
sure corresponding to the axial component of the exit velocity
computed from continuity considerations. The weight flow of air
was determined from the orifice measurements together with the
data of reference 5. This method of computing the exit total pres-
sure gives a minimum value because any energy available from the
tangential component of the velocity is neglected.

The brake net efficiency, which is based on expansion between
the entrance total and exit static pressures, is defined as

$$\eta_{net} \equiv \frac{E}{\left(h'_1 - h_4\right)_s}$$

The ideal drop in enthalpy $\left(h'_1 - h_4\right)_s$ was computed from the chart
of air properties in reference 4, the values of inlet total pres-
sure and temperature, and the value of exit static pressure.

Arithmetic averages of the following measurements were used:

(1) Entrance total temperature, four thermocouples in the pair of ducts leading to the plenum chamber

(2) Exit total temperature, three thermocouples at downstream end of exhaust-guide shells

(3) Exit static pressure, twelve wall taps, six in the outer exhaust-guide shell and six in the inner-exhaust guide shell

The ideal jet velocity V_j is the jet speed for an isentropic expansion from the entrance total state to the exit static pressure, that is,

$$V_j \equiv \sqrt{2Jg \ (h'_1 - h_4)_s}$$

All turbine performance data were reduced to NACA sea-level air conditions at the turbine entrance. The performance was expressed in terms of the following variables:

(1) Brake internal efficiency, η_i

(2) Brake net efficiency, η_{net}

(3) Total-pressure ratio, p'_1/p'_4

(4) Equivalent turbine-shaft work, $E(a_0/a'_1)^2$

(5) Ratio of equivalent mean blade speed to equivalent weight flow, $(\rho'_1/\rho_0) \ (U/w)$

(6) Ratio of mean blade speed to ideal jet velocity (blade-to-jet speed ratio), ν

(7) Equivalent mean blade speed, $U(a_0/a'_1)$

RESULTS AND DISCUSSION

The relation among the brake internal efficiency, equivalent mean blade speed, and total-pressure ratio is presented in figure 9; the symbols represent actual data points. Because these

data were obtained at varying total-pressure ratios, plots like
that of figure 9 are unsuitable for presenting the complete per-
formance; therefore, curves of constant equivalent mean blade
speed were faired through the computed data points and cross-
plotted to present the other performance results.

The over-all turbine performance is presented in figure 10,
which is a plot of the equivalent turbine-shaft work against the
ratio of equivalent mean blade speed to equivalent weight flow,
with equivalent mean blade speed and total-pressure ratio as param-
eters and with contours of brake internal efficiency. The brake
internal efficiency had a maximum value slightly greater than 0.84
in the region of the design point, for which the pressure ratio
and blade speed were relatively high. Another region of high effi-
ciency occurred at pressure ratios less than 1.50 and equivalent
mean blade speeds from 300 to 400 feet per second. A maximum effi-
ciency of 0.85 occurred in this region but the pressure ratio and
consequently the work output were far below the design values. A
brake internal efficiency of 0.81 was obtained over the entire
range of total-pressure ratios from 1.25 to 3.80. At the equivalent
mean blade speed and total-to-static pressure ratio for which the
blades were designed, the total-pressure ratio was 3.26; at this
point the brake internal efficiency was greater than 0.82, which is
0.10 lower than the design value. The actual total-pressure ratio
corresponding to the design total-to-static pressure ratio of 4.00
was 3.26 instead of the design value of 3.32 because three operating
conditions that differed from the design conditions influenced the
exit static-to-total pressure ratio: (1) the weight flow, (2) the
exit total temperature, and (3) the ratio of specific heats. For
a set value of the total-to-static pressure ratio, the total-
pressure ratio is decreased for increased values of weight flow and
exit total temperature, but is increased for increased values of
the ratio of specific heats. The actual weight flow was greater
than the design value. Because the efficiency was lower than the
design value, the exit total temperature was higher than for the
predicted value. The ratio of specific heats was about 1.400
instead of the design value of 1.300. Because the effect of the
greater weight flow and exit total temperature overbalanced the
effect of the change in the ratio of specific heats, the actual
total-pressure ratio was lower than the design value.

At the total-pressure ratio of 3.26, the region of highest
efficiency occurred at equivalent mean blade speeds about 15 percent
higher than the design value of 643 feet per second. The increase
in brake internal efficiency with higher blade speeds may be attri-
buted to two factors: (1) At the design blade speed, the exit

tangential component of the velocity was appreciable; as the blade speed was increased, the magnitude of this tangential velocity component and the loss associated with it were diminished; and (2) as the blade speed was increased, the angle of attack at the rotor entrance became smaller. The design angle of attack may have been too large for highest efficiency.

The lines of constant equivalent mean blade speed are vertical above a total-pressure ratio of approximately 2.25 because at these pressure ratios the stator was choking, which resulted in a constant value of the ratio of equivalent mean blade speed to equivalent weight flow along the blade-speed curves. At total-pressure ratios less than 2.25, this ratio increased along lines of constant blade speed because the weight flow decreased. At the design point, the equivalent weight flow was 5.97 pounds per second, 2.6 percent greater than the design value.

The variation of the brake internal efficiency with the blade-to-jet speed ratio is shown in figure 11 for total-pressure ratios of 1.50 and 3.50. The highest values of brake internal efficiency were obtained at blade-to-jet speed ratios between 0.48 and 0.55. These values were higher than the design blade-to-jet speed ratio of 0.43 because of the reduction in the exit loss as the blade speed was increased above the design value. Blade-to-jet speed ratios greater than 0.55 were unattainable at a total-pressure ratio of 3.50 because of blade-stress limitations. In general, these curves were insensitive to changes in total-pressure ratio.

The brake internal and brake net efficiencies are compared in figure 12 for total-pressure ratios of 1.50 and 3.50. At a total-pressure ratio of 1.50, the brake net efficiency was about 91 percent of the brake internal efficiency, whereas at a total-pressure ratio of 3.50 the ratio of efficiencies was about 0.86. Over the range of blade-to-jet speed ratios, the ratio of the two efficiencies remained practically constant for a given total-pressure ratio because the ratio of exit static-to-total pressures varied only slightly with blade-to-jet speed ratio. The difference between the two efficiencies increased as the total-pressure ratio was increased because at the high total-pressure ratios the large volume of exhaust gas produced high exit velocities and consequently a large difference between the exit total and static pressures. The maximum values of brake net efficiency were obtained at blade-to-jet speed ratios between 0.48 and 0.55.

The relation of brake net efficiency and total-pressure ratio for a blade-to-jet speed ratio of 0.54, at which the brake net

efficiency reached its maximum value, is presented in figure 13.
At a total-pressure ratio of 2.70, the brake net efficiency reached
the maximum of 0.76.

Although the turbine design assumed constant static pressure
along the radius at the entrance and the exit of each row of blades,
this assumption was not satisfied in the actual turbine. This
deviation from the design occurred because the design assumption of
constant static pressure along the radius neglected the radial
forces required to make a fluid flow along a cylindrical surface
when high tangential velocities are involved. A measure of the
deviation of the actual flow from the design flow may be obtained
by comparing the exit static pressures measured at the inner and
outer radii. The variation of the static-to-total pressure ratios
at the inner and outer radii with total-pressure ratio for the design
equivalent mean blade speed is shown in figure 14. The static pres-
sure at the inner radius was consistently lower than the static pres-
sure at the outer radius. At a total-pressure ratio of 3.26, the
average of the two static-to-total pressure ratios was 0.25, which
is the design value, and the variation between the pressures was
about 5 percent. The pressure variation at the rotor entrance was
probably greater than 5 percent because of the higher tangential
velocities.

SUMMARY OF RESULTS

A set of turbine blades was designed for 40-percent reaction
and a total-to-static pressure ratio of 4.00 based on the assumption
of constant static pressure along the radius and one-dimensional-
flow theory for the design of the rotor-blade passages. An inves-
tigation of this design in an experimental cold-air turbine yielded
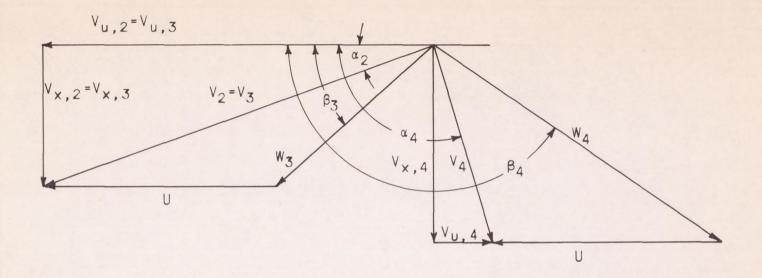the following results:

1. The maximum brake internal efficiency in the region of the
design point was slightly greater than 0.84.

2. A brake internal efficiency of 0.81 was obtained over the
entire range of total-pressure ratios investigated from 1.25 to 3.80.

3. At the equivalent mean blade speed and total-to-static pres-
sure ratio for which the blades were designed, the brake internal
efficiency was greater than 0.82 and the equivalent weight flow was
2.6 percent greater than the design value.

4. The maximum values of both the brake internal efficiency
and the brake net efficiency were obtained with blade-to-jet speed
ratios between 0.48 and 0.55.

5. Measured static pressures in the exhaust annulus showed
that, contrary to the design assumption, the static pressure varied
from root to tip by 5 percent at the design conditions.

Lewis Flight Propulsion Laboratory,
    National Advisory Committee for Aeronautics,
        Cleveland, Ohio.

<div align="center">REFERENCES</div>

1. Church, Edwin F., Jr.: Steam Turbines. McGraw-Hill Book Co.,
    Inc., 2d ed., 1935, pp. 145, 146.

2. Warren, G. B., and Keenan, J. H.: A Machine for Testing Steam-
    Turbine Nozzles by the Reaction Method. Trans. A.S.M.E.,
    vol. 48, 1926, pp. 33-59; discussion, pp. 59-64.

3. English, Robert E., McCready, Robert J., and McCarthy, John S.:
    Some Effects of Stator Cone Angle and Blade-Tip Leakage on
    40-Percent-Reaction Turbine Having Rotor-Blade Caps. NACA RM.
    E8I21, 1949.

4. Amorosi, A.: Gas Turbine Gas Charts. Res. Memo. No. 6-44
    (Navships 250-330-6), Bur. Ships, Navy Dept., Dec. 1944.

5. Anon.: Fluid Meters, Their Theory and Application. A.S.M.E.
    Res. Pub., Am. Soc. Mech. Eng. (New York), 4th ed., 1937.

$V_{u,2} = V_{u,3}$

$V_{x,2} = V_{x,3}$ $V_2 = V_3$ β_3 α_2

W_3 α_4 W_4

$V_{x,4}$ V_4 β_4

U

$V_{u,4}$

U

Velocity (ft/sec)		Angle (deg)	
V_2	2166	α_2	20.0
V_4	1281	α_4	113.2
$V_{u,4}$	506	β_3	41.9
$V_{x,4}$	1177	β_4	145.5
U	1210		
W_3	1110		
W_4	2081		

NACA

Figure 1. — Velocity-vector diagram for mean section of blade for design reaction of 40 percent.

Air flow

1.150

0.031 rad

B

A

0.375 rad

0.057

1.075 rad

0.970

1.474

2.000 rad

C

0.322

0.062

20°

1.125

0.031

1.100

0.200

D

NACA
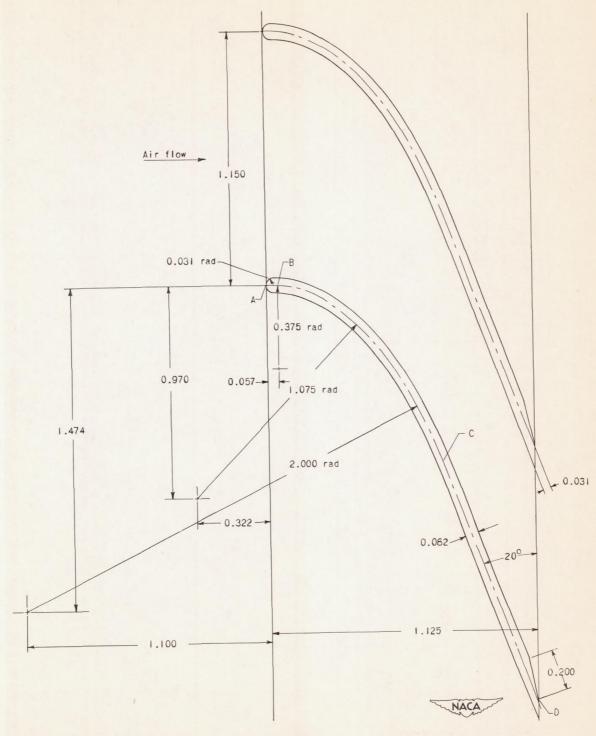
Figure 2. – Construction of stator-blade profile (mean section). (All dimensions in in.)

Air flow

14°

24°

14.60"
diam.

11.73"
diam.

1.125"

NACA
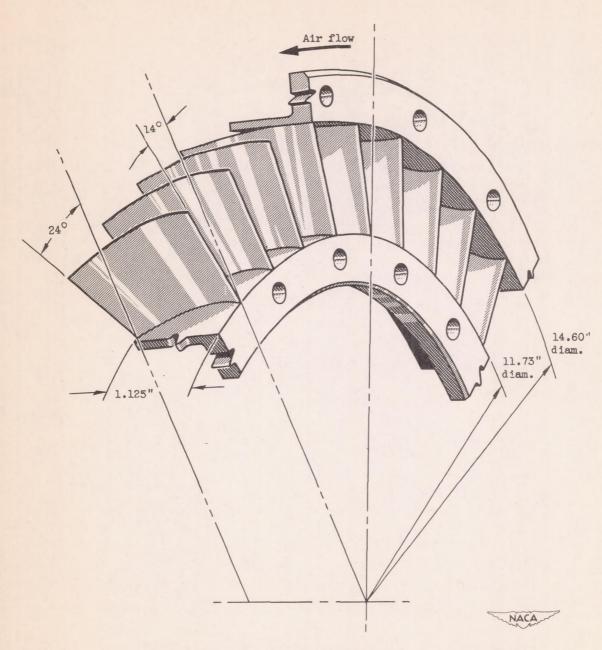
Figure 3. - Stator assembly showing setting of blades and annulus dimensions.
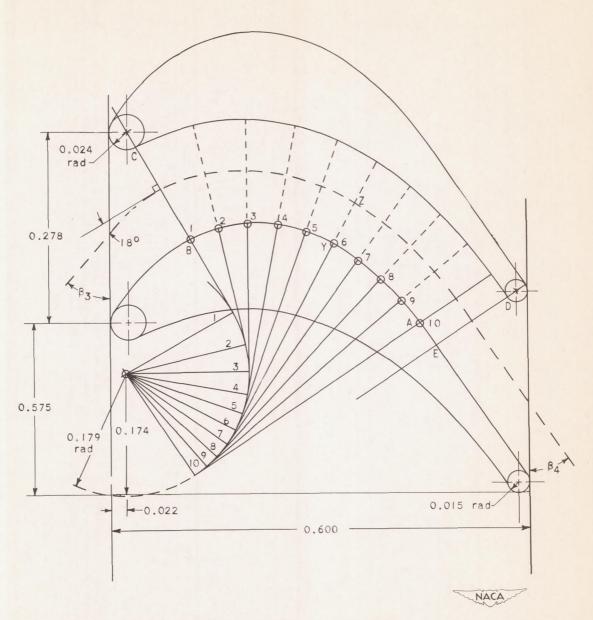
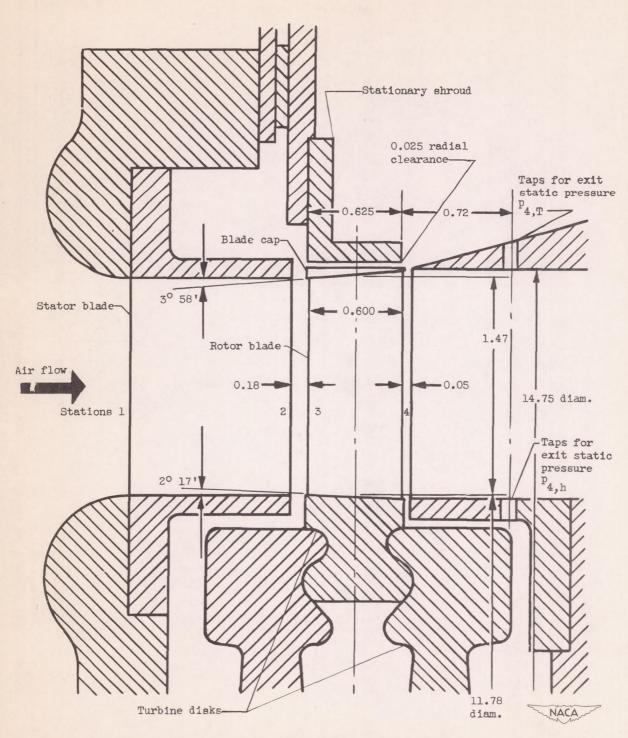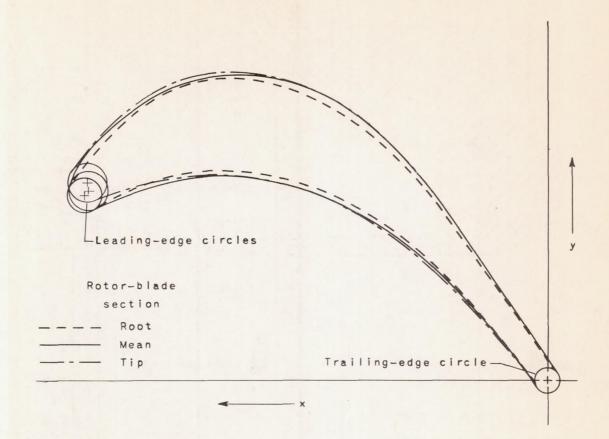Figure 4. — Method of construction of rotor—blade profile (mean section). (All dimensions in in.)

Stationary shroud

0.025 radial
clearance

Taps for exit
static pressure
$p_{4,T}$

0.625   0.72

Blade cap

3° 58'   0.600

Stator blade

Rotor blade   1.47

Air flow

0.18   0.05

Stations 1   2   3   4   14.75 diam.

2° 17'   Taps for
exit static
pressure
$p_{4,h}$

Turbine disks   11.78
diam.

NACA

Figure 5. - Sketch of turbine-blading configuration showing turbine dimensions. (All
dimensions in in.)

Leading-edge circles

Rotor-blade
section
- - - -   Root
———   Mean
-· - ·   Tip

Trailing-edge circle

y

x

	Position of leading-edge circle (in.)		Radius of circle (in.)	
	x	y	Leading edge	Trailing edge
Root	0.565	0.229	0.020	0.015
Mean	.560	.234	.024	.015
Tip	.561	.244	.023	.015

Figure 6. – Superimposed root, mean, and tip
sections of rotor blade.
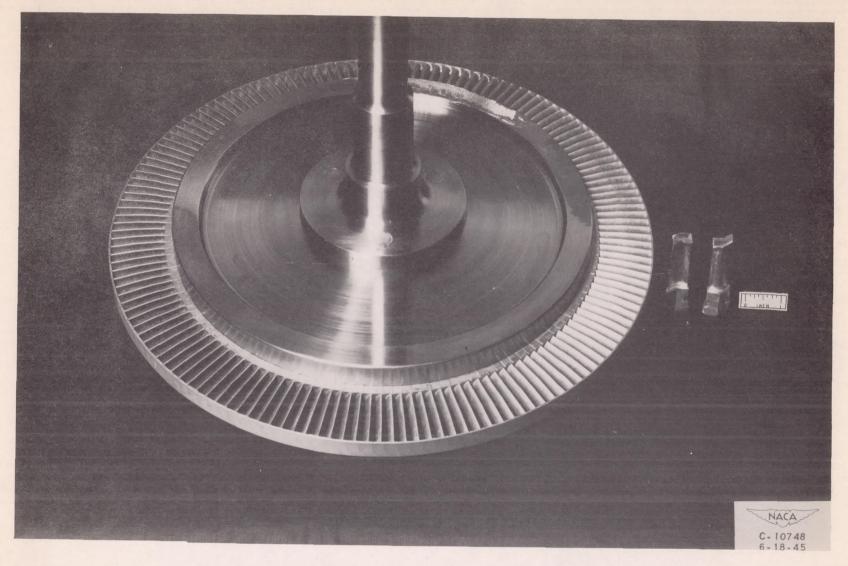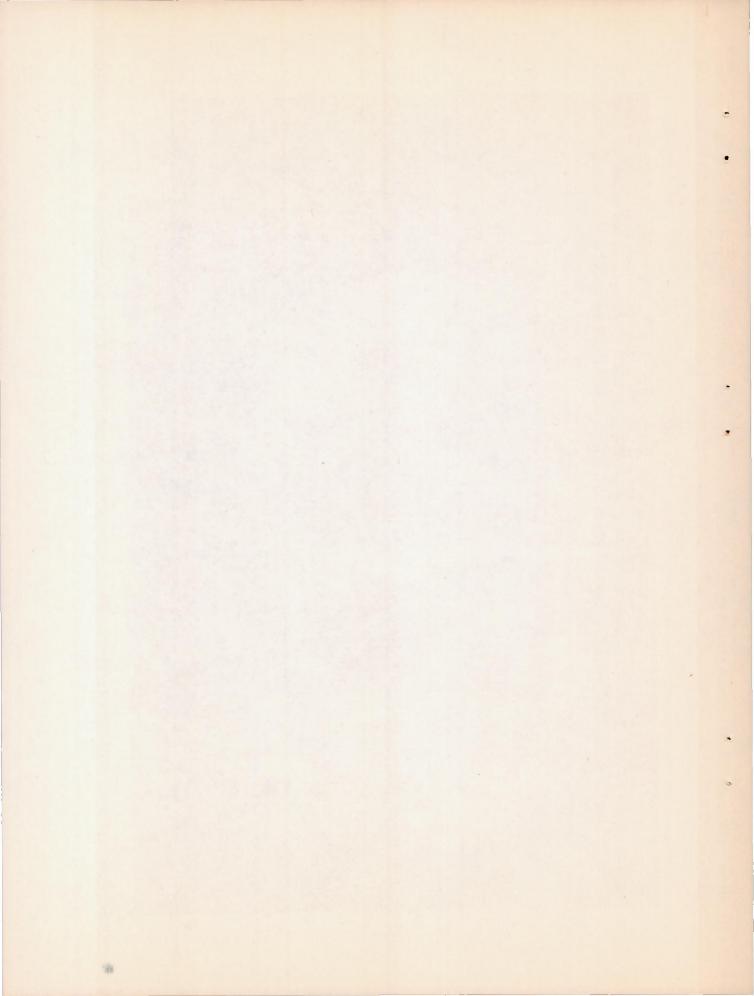
Figure 7. - Assembled rotor showing rotating shroud formed by blade caps.

Thermocouples for entrance
total temperature T'_1

Tube for entrance
total pressure p'_1

Stator blade

Rotor blade

Air
flow — Screen

Taps for exit
static pressure
$p_{4,T}$

Tail pipe

Outer exhaust-guide shell

Thermocouple for exit
total temperature T'_4

1 2 3 4   Stations

Air flow

.75"

Inner exhaust-guide shell

Straightening grid

Taps for exit
static pressure
$p_{4,h}$

Turbine disks

NACA

Rotor assembly

Figure 8. - Cross section of turbine assembly showing instrumentation.
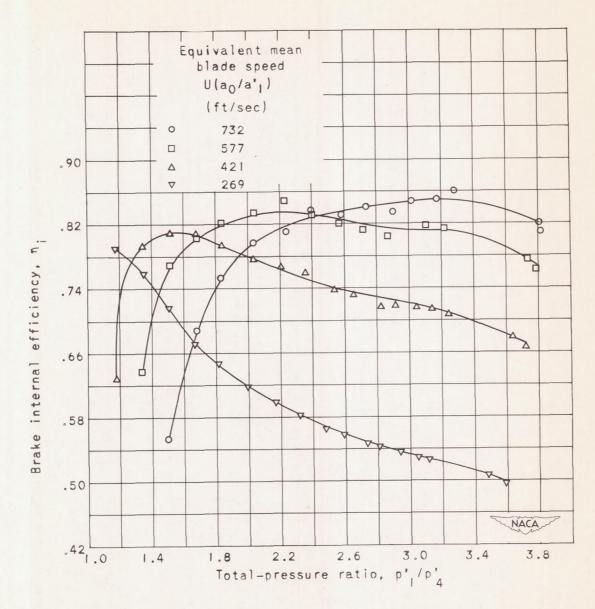
Figure 9. – Variation of brake internal efficiency with blade speed and total-pressure ratio.
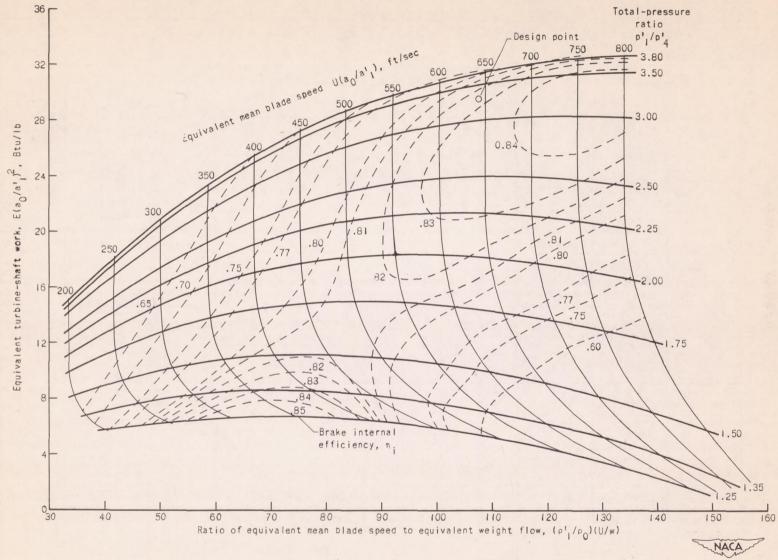
Figure 10. - Over-all turbine performance.
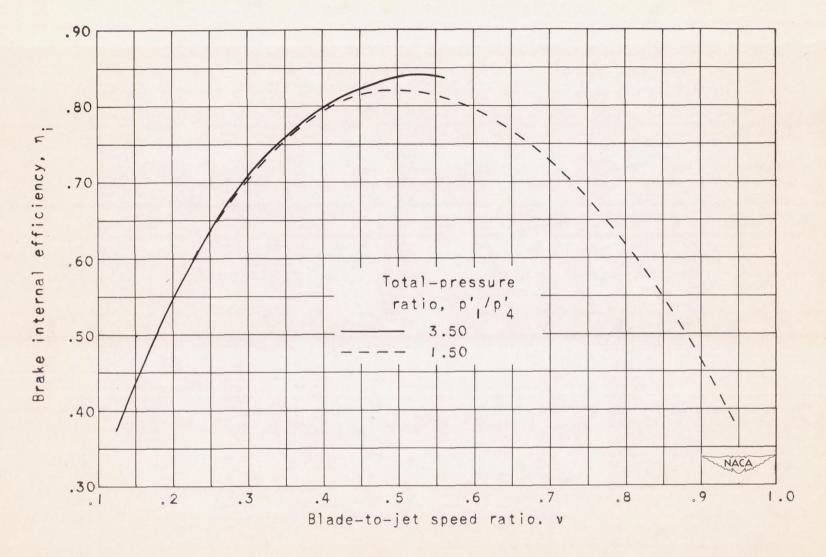
Figure 11. — Variation of brake internal efficiency with blade-to-jet speed ratio.
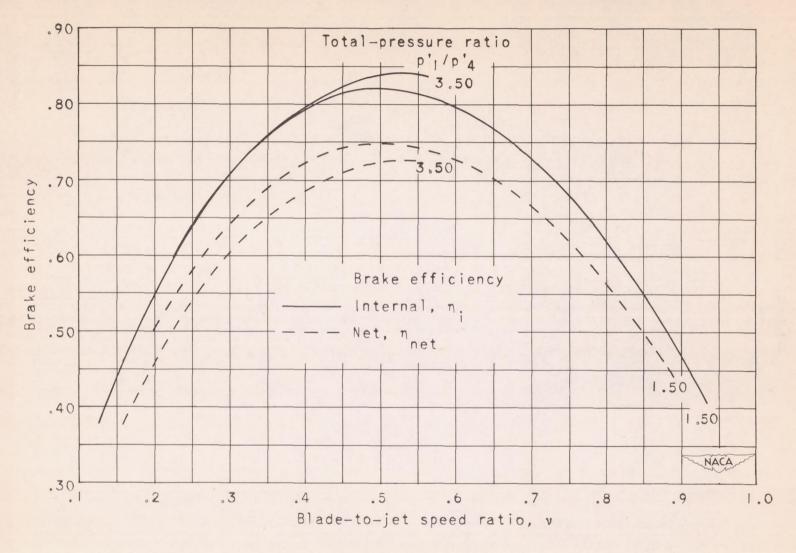
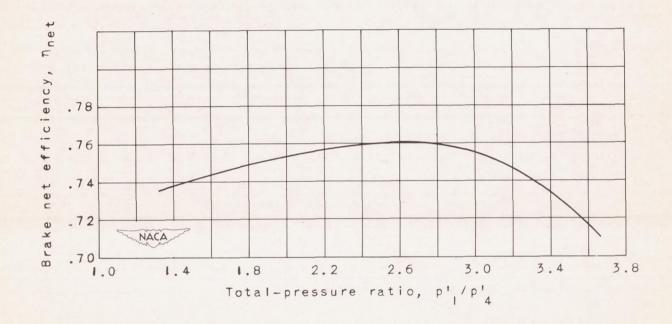Figure 12. – Comparison of brake internal and brake net efficiencies.

Figure 13. - Variation of brake net efficiency with total-pressure ratio. Blade-to-jet speed ratio, 0.54.
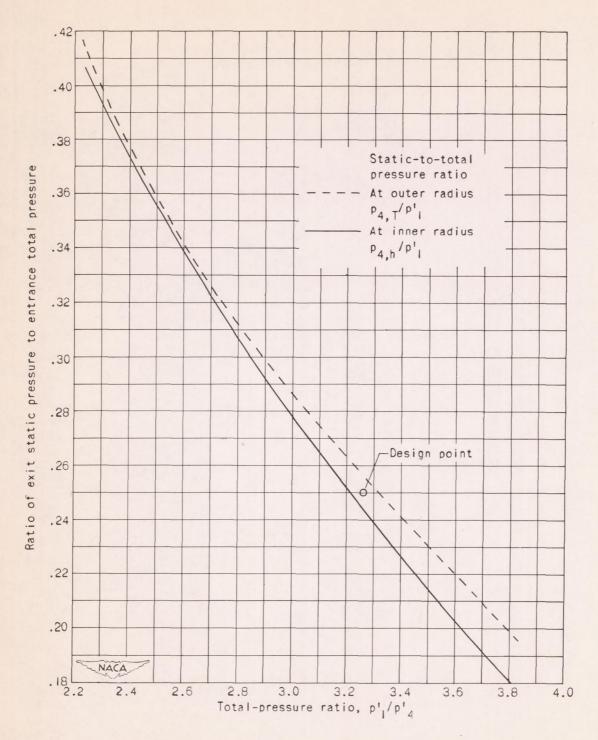
Figure 14. – Comparison of static pressures at inner and outer radii
of annulus at rotor exit.